*Article*

# $D_3$ dihedral logistic map of fractional order

**Marius-F. Danca** [ID] **1*** **and Nikolay Kuznetsov** **2**

1 Babes-Bolyai University, Cluj-Napoca,
STAR-UBB Institute, 400084, Cluj-Napoca, Romania
and
   Romanian Institute of Science and Technology, 400504, Cluj-Napoca, Romania;
danca@rist.ro
2 Saint-Petersburg State University, Russia
and
University of Jyväskylä, Finland;
nkuznetsov239@gmail.com
*    Correspondence: danca@rist.ro (RO)

**Abstract:** In this paper the $D_3$ dihedral logistic map of fractional order is introduced. The map presents a dihedral symmetry $D_3$. It is numerically shown that the construction and interpretation of the bifurcation diagram versus the fractional order require special attention. The system stability is determined and the problem of hidden attractors is analyzed. Also, analytical and numerical results show that the chaotic attractor of integer order, with $D_3$ symmetries, looses its symmetry in the fractional-order variant.

## 0. Introduction

Fractional calculus, a branch of mathematical analysis, is used to model many processes for which the standard integer-order derivatives do not work adequately. The derivative of non-integer order dates back to the beginning of the theory of differential calculus (letter of Gottfried Wilhelm Leibniz, 1695). The rapid development of the theory of fractional calculus started from the work of Euler, Liouville, Riemann, Letnikov, and so on [31,32].

As mentioned in [11], it is well known that the classical derivative of a continuous-time periodic function is a periodic function with the same period. However, with respect to derivative of fractional order, this is different because the periodicity is not necessarily maintained by fractional derivative of periodic functions [2,20,26,27,36,38,39,43]. The non-periodicity of solutions in continuous systems of fractional order (FO) was first discovered by engineers (see e.g. [39]), and then proved by mathematicians (see e.g. [2,26]). Just like for continuous FO systems, the periodicity aspects in discrete FO systems became an important issue [4,17–20,25,33].

In this paper, the numerically orbits which apparently indicate some regular behavior are called periodic-like orbits. It is also well known that in the theory of dynamical systems, every emerging abrupt period-doubling is considered as bifurcation. Therefore, in this paper the term *bifurcation* or *bifurcation diagram* is understood in the above sense of a periodic-like phenomenon.

From a computational point of view, and based on the complexity or simplicity in finding a basin of attraction in the phase space, it is natural to consider the following classification of attractors: self-excited attractors, which can be revealed numerically by integrating the systems with initial conditions within small neighborhoods of unstable equilibria, and hidden attractors, which have the basins of attraction not connected with any equilibria [13,28–30]. Examples of hidden attractors in continuous-time FO

systems exist in systems such as Hopfield neuronal system [8], economic system [15], hyperchaotic discontinuous system [12], and so on [24]. Problems of discrete systems of FO, such as hidden attractors and chaos control are analyzed in [11] and [9,10,14] respectively.

On the other side, as known, a dihedral group is a group of symmetries of a regular polygon (a plane closed polygonal curve with all line segments with the same length and interior angles with same measure) including rotations and reflections [42]. In geometry by $D_m$ one denote the symmetries of a regular $m$-gon, which form a group of order $2m$. The dihedral group is generated by two elements: reflection $S$ in the symmetry axes and rotation $R$ about the center of the polygon with an angle $\theta = 360^0/m$ in the counterclockwise direction. This group can be considered as generated by combining rotations and mirror reflections several times. For $m = 3$ the group is called the symmetry group of the equilateral triangle. An example of a $D_3$ group is the Mercedes-Benz symbol. The operation within the group is the composition of symmetries $S$ and $R$. For a map $f : \mathbb{C} \to \mathbb{C}$ with symmetry $D_m$ one have

$$\begin{aligned} f[S(z)] &= S[f(z)] \\ f[R(z)] &= R[f(z)] \end{aligned} \tag{1}$$

In this paper is presented a FO variant of one of $D_3$ dihedral maps, called $D_3$ dihedral logistic map. Integer order (IO) variants have been introduced by Golubitsky's [7,21,22] (see also [35]). Parameters are fixed and the fractional order is varied to study the underlying dynamics.

The structure of the paper is as follows: In Section 1 the dihedral logistic map of IO is presented; In Section 2 the FO variant of the system is deduced; Section 3 deals with the numerical integration of the FO variant; In Section 4 the problems related to the bifurcation diagrams are analyzed; Section 5 deals with the hidden attractors and in Section 6 the symmetry breaking is analyzed, while the paper is ended with the Conclusion section.

## 1. $D_3$ dihedral logistic map of IO

The beauty of the symmetry groups can be unveiled better in the complex plane that in the cartesian plane as it is simplest to work with complex numbers. Consider a map $f : \mathbb{C} \to \mathbb{C}$, $z = x + iy \in \mathbb{C}$ and the iteration

$$z_n = f(z_{n-1}), \quad z_0 = x_0 + iy_0 \in \mathbb{C}, \quad n \geq 1. \tag{2}$$

One of the Dihedral Logistic Maps (DLMs) [7,21,22] (see also [35]), is defined as

$$f(z) = (\alpha + \beta z\bar{z} + \gamma \Re(z^m))z + \delta \bar{z}^{m-1},$$

with $\alpha, \beta, \gamma, \delta$ as real parameters. Due to particular symmetries, this systems belongs to the maps with $D_m$ symmetries and is also called the $D_m$ *dihedral logistic map*.

Consider the case of $m = 3$. After some calculations one obtains the following form for $f$

$$f(x,y) := \begin{pmatrix} f_1(x,y) \\ f_2(x,y) \end{pmatrix} = \begin{pmatrix} \alpha x + (x^3 + xy^2)\beta + (x^4 - 3x^2y^2)\gamma + \delta(x^2 - y^2) \\ \alpha y + (x^2y + y^3)\beta + (x^3y - 3xy^3)\gamma - 2\delta xy \end{pmatrix}. \tag{3}$$

Thus, in the cartesian parametric form , the iteration (2) defining the DLM of IO is

$$x_n = \alpha x_{n-1} + (x_{n-1}^3 + x_{n-1} y_{n-1}^2)\beta + (x_{n-1}^4 - 3x_{n-1}^2 y_{n-1}^2)\gamma + \delta(x_{n-1}^2 - y_{n-1}^2),$$

$$y_n = \alpha y_{n-1} + (x_{n-1}^2 y_{n-1} + y_{n-1}^3)\beta + (x_{n-1}^3 y_{n-1} - 3x_{n-1} y_{n-1}^3)\gamma - 2\delta x_{n-1} y_{n-1}, \quad (4)$$

$$n \geqq 1, \ x_0, y_0 \in \mathbb{R}.$$

In this paper one chose for (4) the particular case: $\alpha = -1.8040$, $\beta = 1$, $\gamma = 0$ and $\delta = 0.5$, values for which the system becomes

$$x_n = -1.8040\, x_{n-1} + x_{n-1}^3 + x_{n-1} y_{n-1}^2 + 0.5\, x_{n-1}^2 - 0.5\, y_{n-1}^2,$$

$$y_n = -1.8040\, y_{n-1} + y_{n-1} x_{n-1}^2 + y_{n-1}^3 - x_{n-1} y_{n-1}, \quad (5)$$

$$n = 1, 2, ..., \ x_0, y_0 \in \mathbb{R}.$$

The image of the attractor obtained after 10000 iterations is presented in Fig. 1.

## 2. Dihedral logistic map of FO

Consider the Caputo's like discrete Initial Value Problem of FO with $q \in (0, 1)$ and starting point 0:

$$\Delta_*^q u(t) = f(t + q - 1), u(t + q - 1)), \ t \in \mathbb{N}_{1-q}, \ u(0) = u_0, \quad (6)$$

where $N_a = \{a, a + 1, a + 2, \dots\}$ and $\Delta_*^q$ stands as the $q$-th Caputo-like discrete fractional difference. Then, with $f$ given by (3) in the scalar form (5), the DLM of FO (called DLMFO hereafter) is expressed as follows

$$\Delta_*^q x(t) = \alpha x(t + q - 1) + (x^3(t + q - 1) + x(t + q - 1)y^2(t + q - 1))\beta +$$

$$\qquad (x^4(t + q - 1) - 3x^2(t + q - 1)y^2(t + q - 1))\gamma + \delta(x^2(t + q - 1) -$$

$$\qquad y^2(t + q - 1)),$$

$$\Delta_*^q y(t) = \alpha y(t + q - 1) + (x^2(t + q - 1)y(t + q - 1) + y^3(t + q - 1))\beta + \quad (7)$$

$$\qquad (x^3(t + q - 1)y(t + q - 1) - 3x(t + q - 1)y^3(t + q - 1))\gamma -$$

$$\qquad 2\delta x(t + q - 1)y(t + q - 1)$$

$$\qquad t \in \mathbb{N}_{1-q}, \ x(0) = x_0, y(0) = y_0.$$

The solution of (6) is the following integral [1,3,6]

$$u(t) = u_0 + \frac{1}{\Gamma(q)} \sum_{s=1-q}^{t-q} (t - s - 1)^{(q-1)} f(u(s + q - 1)). \quad (8)$$

A convenable numerical form of (8) can be obtained with the following substitution: $s + q = i$. Then, $(t - s - 1)^{(q-1)}$ becomes

$$(t - s - 1)^{(q-1)} = \frac{\Gamma(t - s)}{\Gamma(t - s - q)} = \frac{\Gamma(t - 1 + q)}{\Gamma(t - s - q + 1)} = \frac{\Gamma(t - i + q)}{\Gamma(t - i + 1)},$$

and, because $t \in \mathbb{N}_1 = \{1, 2, ...\}$, by replacing $t \in \mathbb{N}$ with the usual index $n \in \mathbb{N}$, a convenient iterative numerical form of the integral (8) is

$$u(n) = u(0) + \frac{1}{\Gamma(q)} \sum_{i=1}^{n} \frac{\Gamma(n - i + q)}{\Gamma(n - i + 1)} f(u(i - 1)), \ u(0) = u_0, \ n \in \mathbb{N}. \quad (9)$$

Adapting (9) to the system (7), with the particularization of parameters $\alpha, \beta, \gamma, \delta$ mentioned before, one obtains the following integral

$$x(n) = x(0) + \frac{1}{\Gamma(q)} \sum_{i=1}^{n} \frac{\Gamma(n-i+q)}{\Gamma(n-i+1)} (-1.804\, x(i-1) + x(i-1)^3 +$$

$$x(i-1)y(i-1)^2 + 0.5\, x(i-1)^2 - 0.5\, y(i-1)^2),$$

$$y(n) = y(0) + \frac{1}{\Gamma(q)} \sum_{i=1}^{n} \frac{\Gamma(n-i+q)}{\Gamma(n-i+1)} (-1.804\, y(i-1) + y(i-1)x(i-1)^2 +$$

$$y(i-1)^3 - x(i-1)y(i-1)), \quad [x(0), y(0)]^t = [x_0, y_0]^t, n \in \mathbb{N},$$

or

$$x_n = x_0 + \frac{1}{\Gamma(q)} \sum_{i=1}^{n} \frac{\Gamma(n-i+q)}{\Gamma(n-i+1)} (-1.804\, x_{i-1} + x_{i-1}^3 + x_{i-1}y_{i-1}^2 + 0.5\, x_{i-1}^2 - 0.5\, y_{i-1}^2),$$

$$y_n = y_0 + \frac{1}{\Gamma(q)} \sum_{i=1}^{n} \frac{\Gamma(n-i+q)}{\Gamma(n-i+1)} (-1.804\, y_{i-1} + y_{i-1}x_{i-1}^2 + y_{i-1}^3 - x_{i-1}y_{i-1}),$$

$$n \in \mathbb{N}, \quad x_0, y_0 \in \mathbb{R}.$$

$$\tag{10}$$

**Remark 1.** *Because the uniqueness of a explicit sequence as (10) is automatic, following [37, Definition 1.1.1], equations (10) define a discrete dynamical system of FO, whose behavior fully represents the dynamics of the DLMFO (7).*

### 3. Stability of fixed points

The study of hidden attractors is based on the stability of the fixed points. Compared to IO counterparts, fixed points of the system (9) are not obtained by solving the equation $f(u) = u$, but solving the equation $f(u) = 0$. Therefore, for the DLMFO system modeled by (10), one obtain the following seven equilibria

$$X_0^* = (0,0), \quad X_1^* = (-1.6162, 0), \quad X_2^* = (1.1162, 0),$$
$$X_{3,4}^* = (-0.5581, \pm 0.9667), \quad \text{and} \quad X_{5,6}^* = (0.8081, \pm 1.3996).$$

The Jacobian is

$$J(x,y) = \begin{pmatrix} 3x^2 + x + y^2 - 1.804 & 2xy - y \\ 2xy - y & x^2 - x + 3y^2 - 1.804 \end{pmatrix}.$$

which will be evaluated at the fixed points $X^*$.

Conform to [5, Theorem 1.4], a fixed point of a discrete FO system is asymptotically stable if all its eigenvalues belongs to the set $S^q$:

$$S^q = \left\{ z \in \mathbb{C} : |z| < \left( 2\cos \frac{|\lambda| - \pi}{2 - q} \right)^q \text{ and } |\lambda| > \frac{q\pi}{2} \right\},$$

where $\lambda$ denotes the argument of the eigenvalue and $|\bullet|$ is evaluated for each eigenvalues of the considered fixed point. If one or several fixed point admit eigenvalues not belonging to $S^q$, then the underlying fixed point is unstable.

**Theorem 1.** $X_0^*$ *is unstable for* $q \in (0, \log_2 1.804)$ *and asymptotically stable for* $q \in (\log_2 1.804, 1)$.

**Proof.** Eigenvalues of $X_0^*$ related to both axis $Ox$ and $Oy$ are: $e_{x,y} = -1.804$ with arguments $\lambda_{x,y} = \pi$. The first inequality of $S^q$ becomes:

$$|z| = 1.804 < 2^q \cos^q \frac{0}{2-q} = 2^q,$$

wherefrom one obtains:

$$q > \log_2 1804 \approx 0.8512. \tag{11}$$

The second inequality is:

$$|\lambda_{x,y}| = \pi > \frac{q\pi}{2},$$

wherefrom

$$q < 2. \tag{12}$$

Because in this paper $q \in (0,1)$, from (11) and (12) one obtains $q \in (\log_2 1.804, 1)$. $\square$

**Theorem 2.** $X_{1-6}^*$ *are unstable for* $q \in (0,1)$.

**Proof.** Consider only the points $X_{1,2}^*$, the calculations for the other points following the same path. Eigenvalues of the point $X_1^*$ are $e_x = 4.4161$ and $e_y = 2.4243$ with arguments $\lambda_{x,y} = 0$. Then $|\lambda_{x,y}| = 0 < \frac{q\pi}{2}$ which contradicts the second inequality in $S^q$. Therefore $X_1^*$ is unstable on the plane $(xOy)$.

For $X_2^*$, $e_x = 3.0499$ and $e_y = -1.6743$. Then, $\lambda_x = 0$ and $\lambda_y = \pi$. $|\lambda_x| = 0 < \frac{q\pi}{2}$ which shows $X_2^*$ is unstable along the axis $Ox$. For the axis $Oy$, $|\lambda_y| = \pi$ and the second inequality in $S^q$ gives $q < 2$. Next, the first inequality in $S^q$, where $|z| = 1.6743$, gives the following inequality $1.6743 < 2^q \cos^q \frac{0}{2-q} = 2^q$, wherefrom $q > log_2 1.6743 \approx 0.744$. Therefore, $X_2^*$ is stable along the direction $Oy$ if $q > 0.7446$, but in the plane $(xOy)$, $X_2^*$ is unstable (saddle). $\square$

The position of eigenvalues $e_{x,y}$, related to the stability region $S$ for the range $q \in (0.8152, 1)$, is indicated by the tick line in Fig. 2.

## 4. Bifurcation diagrams

To obtain a visual summary of the dynamics of the DLMFO one considers the Bifurcation Diagram (BD) with respect the fractional order $q \in (0,1)$. As one can see in this section this useful tool should be considered for FO discrete systems with precaution not only due to the mentioned nonexistence of periodic solutions in continuous and also discrete FO systems, but also due to a non-invariance-like with respect to initial conditions (see also [41]). Thus, it is shown empirically that to every considered initial condition corresponds a different diagram which, for avoid the confusion with the BD, will be called Bifurcative Set (BS). So, while for IO discrete systems, such as the logistic map, the BD has a unique shape for whatever initial conditions, in the sense that the diagram obtained for parameter variation has the same shape for whatever initial conditions [16] (see also [34]), the DLMFO has the BD as "composed" of several different BSs, one for each considered initial condition. This characteristic are more evident $q$ values close to 0.

Diagrams in this paper are obtained by integrating the system with five different initial conditions for $n_{max} = 2000$ iterations, from which the first 1700 being discarded to avoid transients. The utilized Matlab code is presented in [16].

Note that for different values of $q$, every considered initial condition in the numerical experiment of the BD, has been iterated before drawing the diagram for $n_{max} = 10000$, in order to verify that the results obtained with $n_{max} = 2000$ are similar to those with $n_{max} = 10000$ iterations, and are not prejudiced by transients. Therefore, the choice of 2000 iterations proved to be an acceptable compromise between computer time and rightness of the results.

For the sake of simplicity, one consider the diagrams for only the variable $x$ (Figs. 3). For figure clarity, only five empirically chosen initial conditions are considered: $[x_0, y_0]_1 = [-0.5, -0.1]$ (magenta), $[x_0, y_0]_2 = [0.2, 0.1]$ (red), $[x_0, y_0]_3 = [.01, .01]$ (blue),

$[x_0, y_0]_4 = [-0.5, 0.3]$ (green), $[x_0, y_0]_5 = [0.1, -0.7]$ (black). Supplementary initial conditions have been tested but the diagrams become too loaded. As can be seen, each initial condition generates a different BS.

Fig. 3 (b) reveals the consistency of the analytical result of the asymptotical stability of $X_0^*$ with the numerical results (point P with $q = 0.8512 \approx \log_2 1.804$). Moreover, the zoom in Fig. 3 (b) shows a periodic-like orbit, which exists for $q < 0.8512$. Figs. 3 (c) and (d) present the time series and phase plot, respectively, indicating the behavior of an orbit starting close from $X_0^*$, which tends asymptotically to $X_0^*$ for $q > 0.8512$.

The following natural questions arise:

$Q_1$: Should the BD be considered as the "reunion" of all BSs?

$Q_2$: Considering the intensive numerical experiments which indicate that different initial conditions generates different BSs, how many such BSs can be finally obtained and which one of these BSs should be considered the "right" BD?

Hereafter, in order to avoid the problem raised by $Q_1$, by BD of the GLMFO one understands the set of all obtained BSs.

Another BD with five initial conditions $[-0.5, 0.1]$ (magenta), $[0.2, 0.1]$ (red), $[-0.01, 0.1]$ (blue), $[.4, .1]$ (green) and $[.1, .1]$ (black), presented in Fig. 4, underlines the differences between BSs, even for $y_0$ kept constant ($y_0 = 01.$).

The following experiment reveals the fact that for any of 600 considered initial conditions $[x_0, y_0]$ within the segment $[x_0, 0.8]$, for $x_0 \in [0.5, 0.5]$, and $q = 0.03$, in the bifurcation diagram vs initial condition, $x_0$ and with $y_0$ constant, there correspond different attractors (Figs. 5 (a)). Because there are an infinity of points within the considered segment, one can extrapolate the idea that to every initial condition there exist different BSs. On the other side, from Fig. 5 (b) one can see that for the IO case of the considered system, the initial conditions $x_0$ give birth to similar (chaotic) attractors. This is in agreement with the cases of IO other discrete and continuous systems where BDs do not present such sensible dependence on initial conditions.

To better understand the differences between the IO cases and FO cases, consider the sketch in Fig. 6, where two BDs are considered. In Fig. 6 (a) is presented a BD of discrete system of IO depending on a real parameter $r$ (such as the logistic map), for a single value of $r$, while in Fig. 6 (b) are presented the BS of a discrete system of fractional order $q$ (like the GLMFO) for a particular value of $q$. Both systems are considered as depending on the variable $u$. The vertical bars or points corresponding to $r$ or $q$ are attractors (Poincaré-like sections of BDs through $r$ or $q$), attractive points or stable cycles (like), quasiperiodic (like) or chaotic attractors. As known, in both cases the chaotic behavior is characterized by the sensitive dependence of initial conditions (as first formulated by Guckenheimer [23]). However, as this paper shows, in FO systems, like the considered GLMFO, for a considered value of $q$ all different initial conditions (in this sketch $u_{0i}$, $i = 1, 2..., 5$), could generate different regular-like, and chaotic attractors (red, yellow, blue, green, black tick lines), while in the IO case all initial conditions lead finally to a single attractor (chaotic in this sketch, black tick line), or two attractors (in the case of multistability).

Therefore, the sensitive dependence of the BD on initial conditions has different meaning from the classical notion of dependence on initial conditions (see [11,16]). Every BD of a FO system, considered as a set of all Poincaré sections through the axis $q$, which are all different, depends sensibly on the considered initial conditions, while every orbit depends sensibly on the initial condition.

**Remark 2.**

*i) Beside the dependence on initial conditions, because fractional derivatives are nonlocal operators, they present the so called memory effect which means that the actual behavior is not only influenced by the actual state of the underlying system but also by the events happened in the past. Therefore, beside the dependence on the initial conditions, at every moment n, the solutions $x_n$ and $y_n$ depends not only on $x_0$ and $y_0$ but also on all previous values $x_k$ and $y_k$, for $k = 1, 2, ..., n-1$.*

ii) *Because the decay rate of the solutions in the asymptotically stable case is $n^{-q}$ [5] (see also [18]), smaller values of q implies bigger errors, while to bigger values of q, close to 1, errors are smaller. In Fig. 7 the graph of $n^{-q}$ is represented as function on n for different values of q. For clarity, only first few dozens of values n have been considered. The circles at $n = 30$ indicates the order of errors for each considered values of q. If one considers $n_{max} = 10000$, from the curve $q = 0.01$ one obtains $10000^{-0.01} = 0.9120$, while the curve $q = 0.9$, gives $10000^{-0.9} = 2.5119e - 004$.*

Consider $q = 0.1$ and the underlying attractors presented in Figs. 8 (see also dotted line in Fig. 3 (b)).

For the initial condition $[x_0, y_0]_1$ one obtains a periodic-like orbit (Fig. 8 (a)), fact underlined by the zoom in phase plane representation (Fig. 8 (b)), which shows the fact that it is not about a true periodic orbit.

For $[x_0, y_0]_2$ one obtains a two-band quasiperiodic-like orbit (Fig. 8 (c)). The two colored filled disks indicate the alternative visiting order of the subsets denoted $\mathcal{A}_1$ and $\mathcal{A}_2$ of the quasiperiodic-like attractor (Fig. 8 (d)). To note that for $q = 0.1$ similar quasiperiodicity-like orbits can be obtained with initial condition within the blue and yellow BSs.

As Fig. 3 (e) shows, there are several bifurcation-like points, the "end" points of quasiperiodic-like behavior of yellow, blue and red BSs (such as the points $P_{1,2}$, $Q_{1,2}$ and $R_{1,2}$ or the point $P$ in Fig. 3 (b)), related to BSs, these points have different positions in the fractional-order space (each of them take place at different values of $q$). Note that, by comparing with the IO case where these points would indicate Hopf bifurcations, in FO systems this is a delicate problem, since periodicity still doesn't exists.

## 5. Hidden attractors

While generally in the cases of IO systems the attractors coexistence, one of the ingredient of hidden attractors, is indicated by the presence of different BSs which seem to coexist and complement each other in a kind of harmony, in the considered case of the DLMFO (and also in some other FO discrete systems, see [11,14,16]) the BSs seem to be independent, having nothing to do with each other.

Let find next the potential hidden chaotic attractors for $q$ within the range $(0, 0.06)$, where the BSs indicate chaotic behavior.

Because for this range of $q$ the fixed points are unstable, one can consider that all chaotic attractors are hidden (see the characterization of hidden attractors in Introduction). As the BSs show (Fig. 3 (a)), there exists periodic chaos, when in the BD, the chaotic attractor consists of several vertical bands and even a typical orbit fills out every of the interval irregularly, the successive iterations visit them periodically.

For example, for $q = 0.03$ and the initial condition $[x_0, y_0]_5$, one obtains the hidden chaotic attractor presented in Fig. 9 (a). The projection on the $Ox$ axis reveals a connected set, as shown by the one-band chaotic segment in the cross-section of the black BS with the line $q = 0.03$. Another hidden chaotic attractor identified in the blue BS, for the initial condition $[x_0, y_0]_3$, which is composed by two disconnected sets (two-band chaotic segments in the cross section of the blue BS with the line $q = 0.03$) is presented in Fig. 9 (b)). If one approaches the zero value of $q$ such as $q = 0.005$, for $[x_0, y_0] = [-0.01, -0.01]$ one obtains another chaotic attractor (Fig. 9 (c)) which resembles with the IO counterpart (Fig. 1).

The numerical experiments show that for $q \in (0, 0.06)$, all BSs give birth hidden chaotic (for $q \in (0, 0.06)$), or periodic-like (for $q \in (0, 1)$), attractors.

As mentioned in $Q_2$ it is difficult to specify the real number of these hidden attractors.

### 6. Symmetry broken by the fractional order

Another interesting property of this system, which probably is due to the fractionality is the fact that, compared with its counterpart IO map, the considered chaotic attractors in Figs. 9 (a),(b) and (c), present a dihedral $D_3$ symmetry-broken.

Consider first the DLM of IO with the typical chaotic attractor depicted in Fig. 1 and the reflection (mirror) lines through the center (origin), $(a), (b), (c)$. As can be seen, (almost) every point can be considered as the mirror with respect one of the axes, or obtained with a rotation. The term "almost" is used due of the iterations convergence.

For example, consider the clear visible point $A$ in Fig. 1 with coordinates $x_A = 0.3216$, $y_A = 0$ and rotate it around the origin $O$ with $R$ (red arrow) with the angle $\theta = 120^0$ counterclockwise. As known, the rotation $R$ in plane can be represented by the matrix

$$R = \begin{pmatrix} \cos(\theta) & -\sin(\theta) \\ \sin(\theta) & \cos(\theta) \end{pmatrix} = \begin{pmatrix} \frac{1}{2} & -\frac{\sqrt{3}}{2} \\ \frac{\sqrt{3}}{2} & \frac{1}{2} \end{pmatrix},$$

and, therefore, the new point, $B$, will have the coordinates

$$\begin{pmatrix} x_B \\ y_B \end{pmatrix} = R \cdot A = \begin{pmatrix} \frac{1}{2} & -\frac{\sqrt{3}}{2} \\ \frac{\sqrt{3}}{2} & \frac{1}{2} \end{pmatrix} \begin{pmatrix} 0.3216 \\ 0 \end{pmatrix} = \begin{pmatrix} -0.1606 \\ 0.2781 \end{pmatrix},$$

with a good approximation of the graphically determined coordinates.

The same point $B$ can be also obtained with a symmetry $S$ across the line $(b)$ (red dotted line). The matrix representation of a symmetry across a line through origin of equation $y = mx$ is (see one of the proofs in [40])

$$S = \frac{1}{1+m^2} \begin{pmatrix} 1 - m^2 & 2m \\ 2m & m^2 - 1 \end{pmatrix}, \tag{13}$$

where $m = \tan \alpha$, $\alpha$ being the angle of line $(b)$ with axis $Ox$, in this case $m = \tan 60^0 = \sqrt{3}$. Therefore,

$$\begin{pmatrix} x_B \\ y_B \end{pmatrix} = S \cdot A = \frac{1}{4} \begin{pmatrix} -2 & 2\sqrt{3} \\ 2\sqrt{3} & 2 \end{pmatrix} \begin{pmatrix} 0.3216 \\ 0 \end{pmatrix} = \begin{pmatrix} -0.1606 \\ 0.2781 \end{pmatrix}.$$

The next result regards the symmetries of the DLMFO.

**Theorem 3.** *Attractors of the DLMFO have not $D_3$ symmetries.*

**Proof.** Consider first the IO and the symmetry $S$ with respect the horizontal axis (symmetry axis $(a)$). Then, because $m = 0$, the symmetry $S$ (13) becomes

$$S = \begin{pmatrix} 1 & 0 \\ 0 & -1 \end{pmatrix}.$$

Applied to some point $(x, y)$ one has

$$S(x, y) = S \begin{pmatrix} x \\ y \end{pmatrix} = \begin{pmatrix} 1 & 0 \\ 0 & -1 \end{pmatrix} \begin{pmatrix} x \\ y \end{pmatrix} = \begin{pmatrix} x \\ -y \end{pmatrix} = (x, -y), \tag{14}$$

and due to the parity of functions $f_{1,2}(x, y)$ in (3) ($f_1$ and $f_2$ are even and odd, respectively), from (1) one obtains

$$f(S(x,y)) = f(x,y)|_{(x,y)=(x,-y)} =$$

$$\begin{pmatrix} -1.8040\,x_{n-1} + x_{n-1}^3 + x_{n-1}y_{n-1}^2 + 0.5\,x_{n-1}^2 - 0.5\,y_{n-1}^2 \\ -1.8040\,(-y_{n-1}) + (-y_{n-1})x_{n-1}^2 + (-y_{n-1})^3 - x_{n-1}(-y_{n-1}) \end{pmatrix} = \begin{pmatrix} f_1(x,y) \\ -f_2(x,y) \end{pmatrix} \tag{15}$$

On the other side

$$S(f(x,y)) = Sf(x,y) = \begin{pmatrix} 1 & 0 \\ 0 & -1 \end{pmatrix} \begin{pmatrix} f_1(x,y) \\ f_2(x,y) \end{pmatrix} = \begin{pmatrix} f_1(x,y) \\ -f_2(x,y) \end{pmatrix}. \tag{16}$$

Therefore, $f(S(x,y)) = S(f(x,y))$. The second condition (1) can be proved similarly.

Consider next the FO case and denote the map of the right hand side of (10) as

$$F(x,y) = \begin{pmatrix} x_0 + F_1(x,y) \\ y_0 + F_2(x,y) \end{pmatrix}, \tag{17}$$

where

$$F_1(x,y) = \frac{1}{\Gamma(q)} \sum_{i=1}^{n} \frac{\Gamma(n-i+q)}{\Gamma(n-i+1)} (-1.804\,x_{i-1} + x_{i-1}^3 + x_{i-1}y_{i-1}^2 + 0.5\,x_{i-1}^2 - 0.5\,y_{i-1}^2),$$

and

$$F_2(x,y) = \frac{1}{\Gamma(q)} \sum_{i=1}^{n} \frac{\Gamma(n-i+q)}{\Gamma(n-i+1)} (-1.804\,y_{i-1} + y_{i-1}x_{i-1}^2 + y_{i-1}^3 - x_{i-1}y_{i-1}),$$

where, for the sake of simplicity, the parameter $n$ and index $i$ in $F_{1,2}$ are omitted.

Following the way used to verify the symmetry for the IO case, by using the parity properties of $F(x,y)$ defined in (17) and following (14) one obtains

$$F(S(x,y)) = F(x,y)|_{(x,y)=(x,-y)} = \begin{pmatrix} x_0 + F_1(x,y) \\ y_0 - F_2(x,y) \end{pmatrix}. \tag{18}$$

On the other side

$$S(F(x,y)) = \begin{pmatrix} 1 & 0 \\ 0 & -1 \end{pmatrix} \begin{pmatrix} x_0 + F_1(x,y) \\ y_0 + F_2(x,y) \end{pmatrix} = \begin{pmatrix} x_0 + F_1(x,y) \\ -y_0 - F_2(x,y) \end{pmatrix}, \tag{19}$$

and, therefore, $F(S(x,y)) \neq S(F(x,y))$.  □

Actually, the explanation of this result lies in the mentioned time history of numerical methods for continuous and also discrete systems of FO. This symmetry broken is also presumably due to the influence of the fractional order $q$ and seems to be more powerful as the $q$ increases. As can be seen from (18) and (19), if $y_0 = 0$, the influence of $y_0$ disappears and symmetry should maintains. However, for $y_0 = 0$, $y_n = 0$ for all $n$ and the attractors starting from $[x_0, 0]$ collapse on the axis $Ox$, case which is not considered here. Thus, while for the hidden chaotic attractors in Figs. 7 (a) and (b) obtained for $q = 0.03$ the symmetry destroyed, the attractor in Fig. 7 (c) with $q = 0.01$ resembles with the its IO counterpart in Fig. 1, but is still non-symmetric.

## 7. Discussion

In this paper one of Golubitsky's maps of IO (dihedral logistic map) has been considered in the FO discrete form. The IO variant presents dihedral $D_3$ symmetry which is lost in the FO variant. It is shown that only few hundreds iteration are not enough to discard transients and to obtain accurate results. As in some previous studied discrete

systems of FO, the bifurcation diagram seems to be composed by several different sets, called bifurcative sets, one for each initial condition, which indicate attractors coexistence. In other words, the bifurcative sets depend sensibly on initial conditions, but in a different sense for the classical meaning of the sensitive dependence on initial conditions of an orbit. Probably due to the convergence of the integration method, for smaller values of $q$, the differences between the bifurcative sets are significant, while for $q$ tending to 1, these sets seem to tend one to each other. The instability of the system and the existence of several bifurcative sets, could be considered ingredient to find hidden attractors. However, finding their exact number, is a difficult if not an impossible task due to the dependence of the bifurcative sets on the initial conditions. One over all, the numerical approach of this system (and probably of other discrete systems of FO) indicates that the tools like bifurcation diagram, or hidden attractors require much more attention.
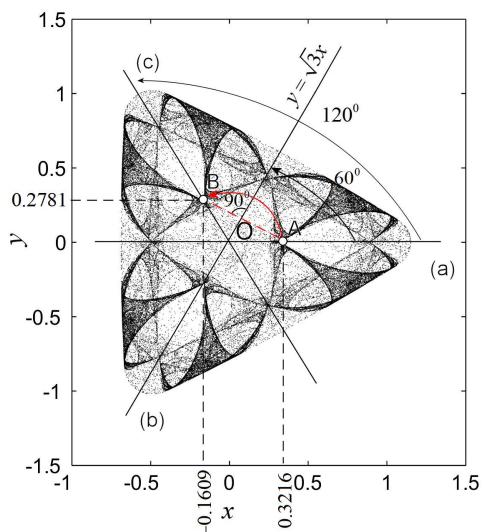
**Figure 1.** A $D_3$-symmetric image of the DLM of IO (5). In red is indicated the counterclockwise rotation with $120^0$ applied to the point $A$ to obtain the point $B$ which is symmetric with respect the line $(b)$.
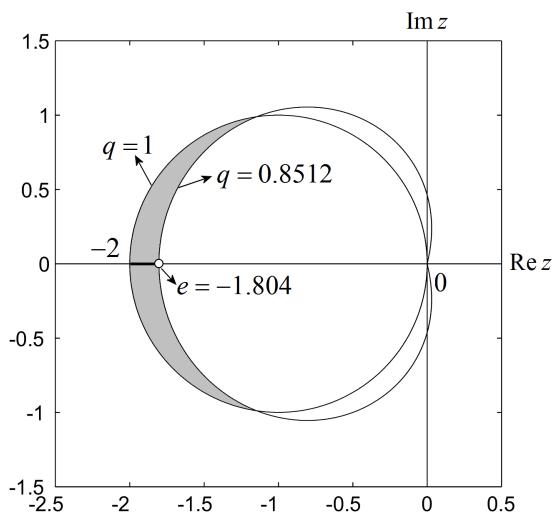
**Figure 2.** Stability domain $S$ in the case of the fixed point $X_0^*$. Tick line represents the asymptoti
stability range of $q$ for $X_0^*$.
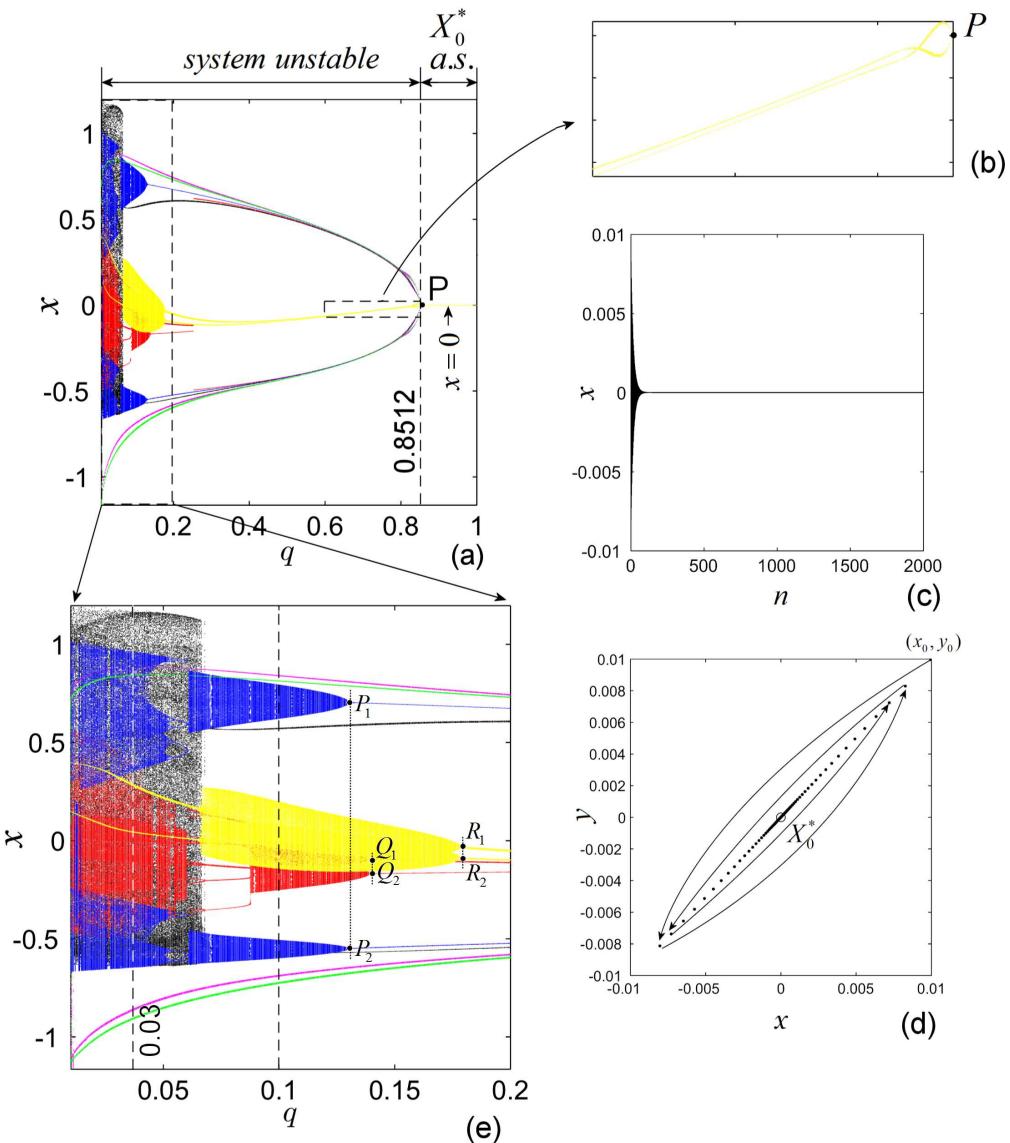
**Figure 3.** DLM of FO. (a) Bifurcation diagram vs $q$. The bifurcation-like point $P$ indicates the beginning of the stability of $X_0^*$ for $q > 0.8512$; (b) Zoomed image; (c) Time series tending to the asymptotically stable fixed point $X_0^*$ for $q > 0.8512$; (d) Phase portrait with the orbit points indicating the evolution of the orbit to $X_0^*$; (e) Zoomed area of the bifurcation diagram.
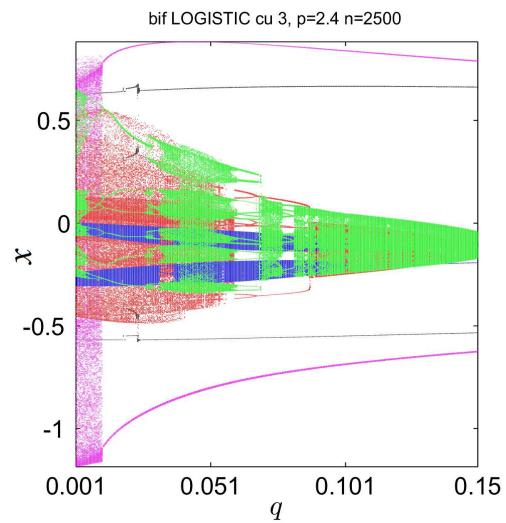
**Figure 4.** Another bifurcation diagram vs $q \in (0, 0.15]$ for initial conditions $[-0.5, 0.1]$, $[0.2, 0.1]$, $[-0.01, 0.1]$, $[0.4, 0.1]$, $[0.1, 0.1]$.
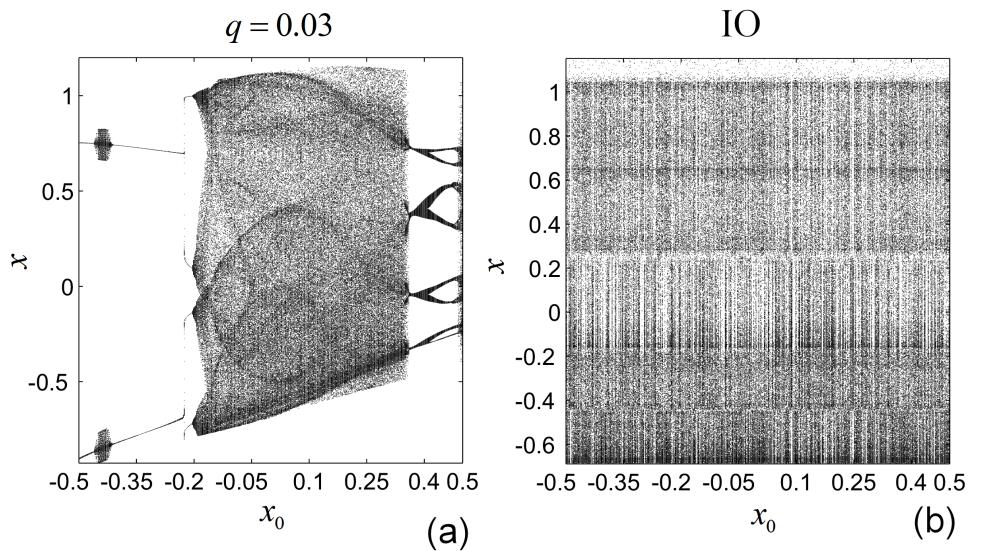


**Figure 5.** Bifurcation diagrams of the DLM of FO and IO versus the initial conditions $x_0 \in [-0.5, 0.5]$ and $y_0 = 0.8$. (a) The FO case $q = 0.03$; (b) The IO case.
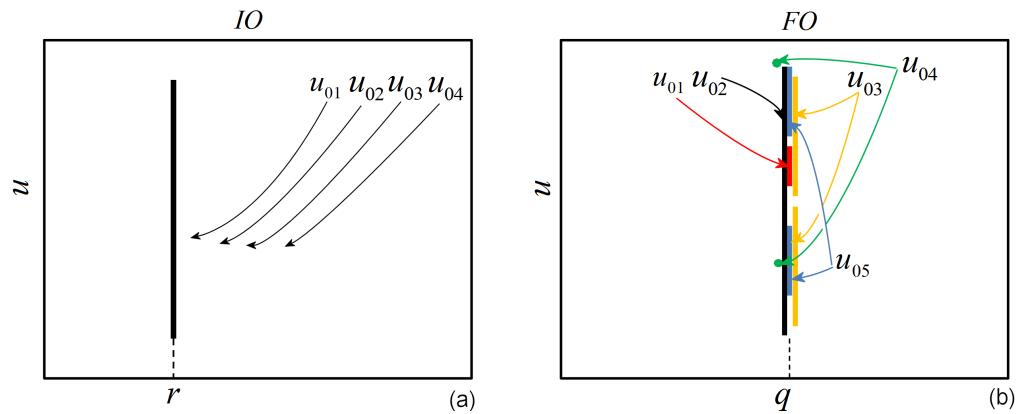
**Figure 6.** Sketch of diagrams of bifurcations. (a) The IO case; (b) FO case. $u_{0i}$, $i = 1, 2, ..., 5$ are initial conditions.
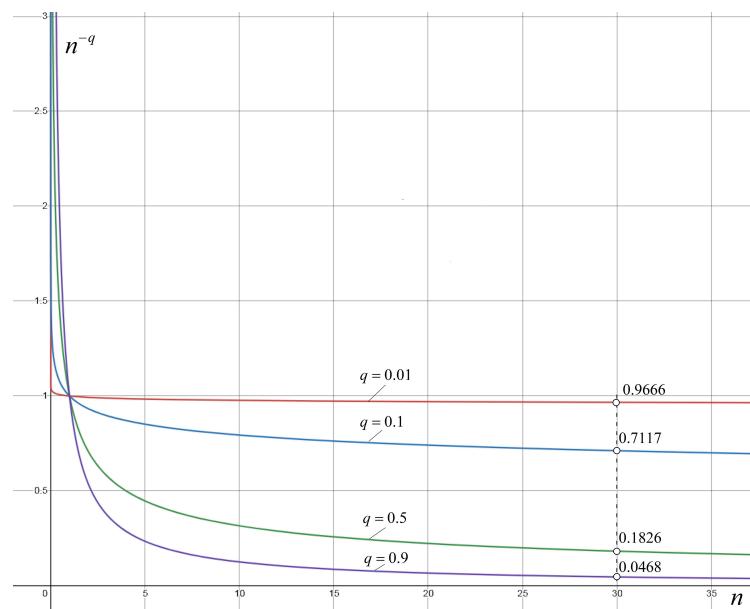


**Figure 7.** Graph of $n^{-q}$ for different values of $q$.
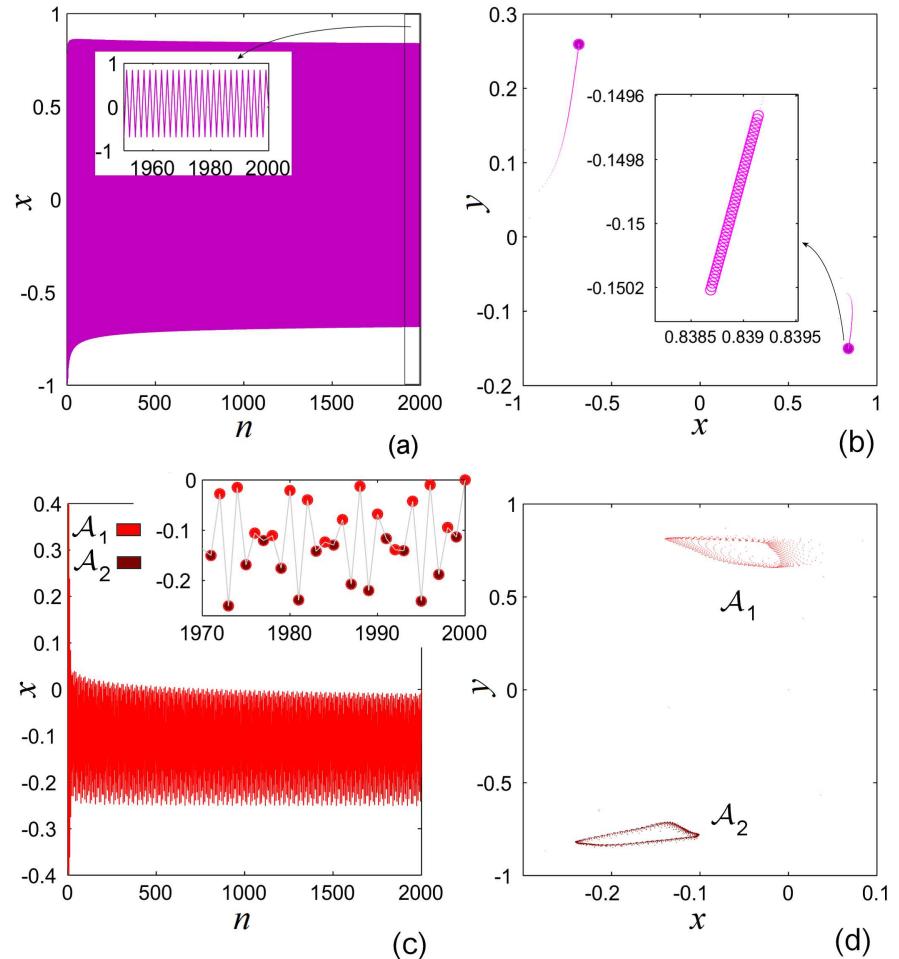
**Figure 8.** Two orbits of the DLM of FO for $q = 0.1$. (a) Time series of a periodic-like orbit from $[x_0, y_0]_1 = [-0.5, -0.1]$; (b) Phase portrait of the orbit and a zoom indicating the slow orbit convergence; (c) Time series of a two-band quasiperiodic-like orbit from $[x_0, y_0]_2 = [0.2, 0.1]$. The zoom indicates the alternate pattern of the orbit between the two subsets $\mathcal{A}_1$ and $\mathcal{A}_2$ (red and brown) of the quasiperiodic-like attractor; (d) Phase portrait of the orbit $[x_0, y_0]_2 = [0.2, 0.1]$.
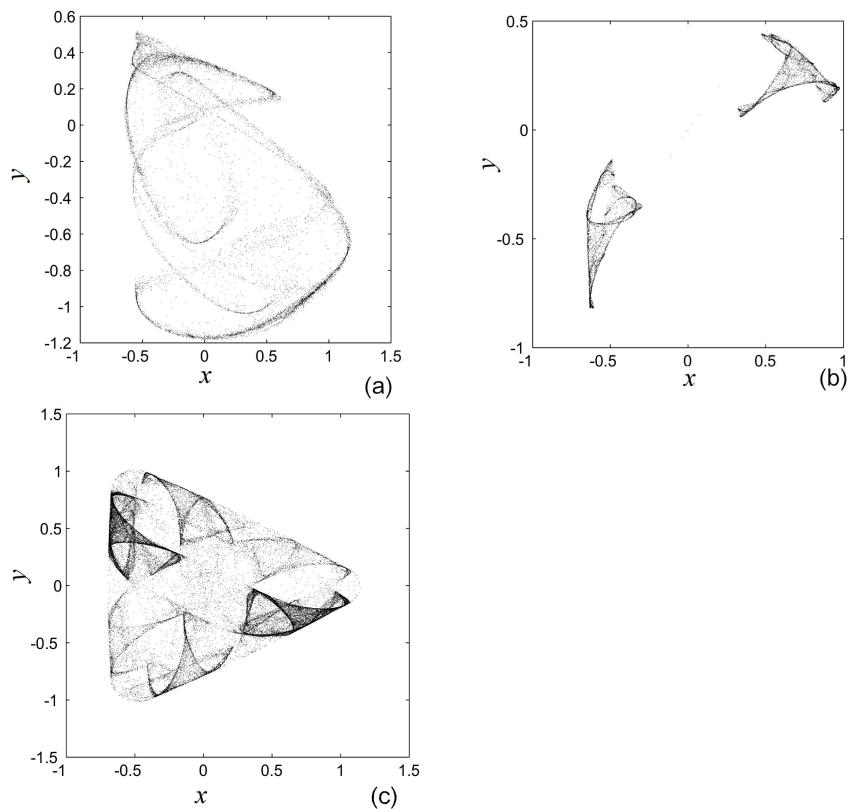
**Figure 9.** Hidden chaotic attractors of the DLMFO with broken-symmetry. (a) $q = 0.03$ and $[x_0, y_0]_5 = [0.1, -0.7]$. (b) $q = 0.03$ and $[x_0, y_0]_3 = [.01, .01]$; (c) $q = 0.01$, and $[x_0, y_0] = [-0.01, -0.01]$.

### 8. Supplementary information

### References

1. Abdeljawad, T. On Riemann and Caputo fractional differences, *Comput. Math. Appl.* **2011** *62*, 1602–1611.
2. Area, I.; Losada, J.; Nieto, J. On Fractional Derivatives and Primitives of Periodic Functions. *Abstr. Appl. Anal.* **2014**, *2014*. art. num. 392598.
3. Atici, F.M.; Eloe, P.W. Initial value problems in discrete fractional calculus. *Proc. Americ. Math. Soc.* **2007**, *137*, 981–989.
4. Bin, H.; Huang, L.; Zhang, G. Convergence and periodicity of solutions for a class of difference systems. *Adv. Differ. Equ.* **2006**, *2006*. art. num. 70461.
5. Čermak, J.; Gyŏri, I.; Nechvátal, L. On explicit stability conditions for a linear fractional difference system. *Fract. Calc. Appl. Anal.* **2015**, *18*, 651–672.
6. Chen F.; Luo X.; Zhou Y. Existence results for nonlinear fractional difference equation *Adv. Differ. Equ.* **2011**, 713201.
7. Chossat P.; Golubitsky M. Symmetry-increasing bifurcation of chaotic attractors, *Physica D* 32 (1988) 423–436
8. Danca, M.F.; Kuznetsov, N. Hidden chaotic sets in a Hopfield neural system. *Chaos, Solitons Fractals* **2017**, *103*, 144–150.
9. Danca, M.-F.; Feckan, M. and Kuznetsov, N. Chaos control in the fractional order logistic map via impulses, *Nonlinear Dyn.* **2019** *98* 1219–1230.
10. Danca, M.-F.; Feckan, M. Chaos suppression in a Gompertz-like discrete system of fractional order, *Int. J. Bifurc. Chaos Appl. Sci. Eng.* **2020** *30* 2050049.
11. Danca, M.-F., Feckan, M. Kuznetsov, N., Chen, G. Coupled Discrete Fractional-Order Logistic Maps, *Mathematics* **2021**, *9*, 2204.
12. Danca, M.F.; Fečkan, M.; Kuznetsov, N.; Chen, G. Complex dynamics, hidden attractors and continuous approximation of a fractional-order hyperchaotic PWC system. *Nonlinear Dyn.* **2018**, *91*, 2523–2540.
13. Danca, M.F. Hidden chaotic attractors in fractional-order systems. *Nonlinear Dyn.* **2017**, *89*, 577–586.
14. Danca, M.F. Puu System of Fractional Order and Its Chaos Suppression. *Symmetry* **2020**, *12*. art. num. 340.
15. Danca, M.F. Coexisting Hidden and self-excited attractors in an economic system of integer or fractional order. *Int. J. Bifurc. Chaos Appl. Sci. Eng.* **2021**, *31*. art. num. 2150062.
16. Danca, M.F. Fractional order logistic map: Numerical approach, **2021** submitted.
17. Diblík, J.; Fečkan, M.; Pospisil, M. Nonexistence of periodic solutions and S-asymptotically periodic solutions in fractional difference equations. *Appl. Math. Comput.* **2015**, *257*, 230–240.
18. Edelman, M. Caputo standard $\alpha$-family of maps: Fractional difference vs. fractional. *Chaos* **2014** *24*, 023137.
19. Edelman, M. On stability of fixed points and chaos in fractional systems. *Chaos* **2018**, *28*. art. num. 023112.
20. Fečkan, M. Note on Periodic and Asymptotically Periodic Solutions of Fractional Differential Equations. in Studies in Systems, Decision and Control, Springer, **2020**, *177*, 153–185.
21. Field, M.; Golubitsky M. *Symmetric Chaos: How and Why*, *Not. Am. math. Soc.* January **1995**.
22. Field, M.; Golubitsky M. *Symmetry in chaos; A Search for Pattern in Mathematics*, Art and Nature 2nd Edition, Philadelphia, PA, Society for Industrial and Applied Mathematics, 2009.
23. Guckenheimer, J. 1979 Sensitive dependence on initial conditions for one-dimensional maps *Commm. Math. Phys. 70*, 133-160.
24. Jafari, S.; Sprott, J.; Nazarimehr, F. Recent new examples of hidden attractors. *Eur. Phys. J. Spec. Top.* **2015**, *224*, 1469–1476.
25. Jonnalagadda, J. Periodic Solutions Of Fractional Nabla Difference Equations. *Communications in Applied Analysis* **2016**, *20*, 585–610.
26. Kang, Y.M.; Xie, Y.; Lu, J.; Jiang, J. On the nonexistence of non-constant exact periodic solutions in a class of the Caputo fractional-order dynamical systems. *Nonlinear Dyn.* **2015**, *82*, 1259–1267.
27. Kaslik, E.; Sivasundaram, S. Non-existence of periodic solutions in fractional-order dynamical systems and a remarkable difference between integer and fractional-order derivatives of periodic functions. *Nonlinear Anal. Real World Appl.* **2012**, *13*, 1489–1497.
28. Kuznetsov, N. Theory of hidden oscillations and stability of control systems. *J. Comput. Sys. Sc. Int.+* **2020**, *59*, 647–668.

29.    Leonov, G.; Kuznetsov, N. Hidden attractors in dynamical systems. From hidden oscillations in Hilbert-Kolmogorov, Aizerman, and Kalman problems to hidden chaotic attractors in Chua circuits. *Int. J. Bifurc. Chaos Appl. Sci. Eng.* **2013**, *23.* art. no. 1330002.

30.    Leonov, G.; Kuznetsov, N.; Mokaev, T. Homoclinic orbits, and self-excited and hidden attractors in a Lorenz-like system describing convective fluid motion. *The European Physical Journal Special Topics* **2015**, *224*, 1421–1458.

31.    Oldham, K.; Spanier, J. *The Fractional Calculus: Theory and Applications of Differentiation and Integration to Arbitrary Order*; Academic Press: New York, 1974.

32.    Podlubny, I. Geometric and physical interpretation of fractional integration and fractional differentiation. *Fract. Calc. Appl. Anal.* **2002**, *5*, 367–386.

33.    Pospíšil, M. Note on fractional difference equations with periodic and S-asymptotically periodic right-hand side. *Nonlinear Oscillations* **2021**, *24*, 99–109.

34.    Prousalis, A.D; Volos, C. K.; Bocheng, B.; Meletlidou, E.; Stouboulos, I. N.; Kyprianidis, I. M. Chapter 6 - *Extreme Multistability in a Hyperjerk Memristive System With Hidden Attractors,* Editor(s): Olfa Boubaker, Sajad Jafari, In Emerging Methodologies and Applications in Modelling, Recent Advances in Chaotic Systems and Synchronization, Academic Press, **2019**, Pages 89–103

35.    Romera, M. Técnica de los sistemas dinámicos discretos (Textos Universitarios) (Spanish Edition) Paperback Consejo Superior de Investigacións Cientificás, January 1, 1997.

36.    Shen, J.; Lam, J. Non-existence of finite-time stable equilibria in fractional-order nonlinear systems. *Automatica* **2014**, *50*, 547–551.

37.    Stuart, A; Humphries, A. R. *Dynamical Systems and Numerical Analysis*, Part of Cambridge Monographs on Applied and Computational Mathematics, Cambridge University Press 1999.

38.    Tavazoei, M.; Haeri, M. A proof for non existence of periodic solutions in time invariant fractional order systems. *Automatica* **2009**, *45*, 1886 – 1890.

39.    Tavazoei, M. A note on fractional-order derivatives of periodic functions. *Automatica* **2010**, *46*, 945–948.

40.    https://yutsumura.com/the-matrix-for-the-linear-transformation-of-the-reflection-across-a-line-in-the-plane/

41.    Wang, Y.; Liu, S.; Li, H. On fractional difference logistic maps: Dynamic analysis and synchronous control. *Nonlinear Dyn.* **2020**, *102*, 579–588.

42.    https://en.wikipedia.org/wiki/Dihedral_group

43.    Yazdani, M.; Salarieh, H. On the existence of periodic solutions in time-invariant fractional order systems. *Automatica* **2011**, *47*, 1834–1837.